Paramagnetic point and pair defects in oxide perovskites — **Source link** ↗

K.A. Müller

Institutions: IBM

Related papers:

- STRONG AXIAL ELECTRON PARAMAGNETIC RESONANCE SPECTRUM OF Fe^{3+} IN SrTiO$_3$ DUE TO NEAREST-NEIGHBOR CHARGE COMPENSATION

- Structure of transition-metal—oxygen-vacancy pair centers

- Electron paramagnetic resonance of three manganese centers in reduced SrTi O 3

- The electronic structure of transition-metal impurities in SrTiO3

- Paramagnetic defects in BaTiO3 and their role in light-induced charge transport. I. ESR studies

Paramagnetic point and pair defects in oxide perovskites

K.A. Müller

Paramagnetic point and pair defects in oxide perovskites (*)

K. A. Müller

IBM Zurich Research Laboratory, Säumerstrasse 4, 8803 Rüschlikon, Switzerland

Résumé. — Le but de cet article est de présenter une synthèse des résultats concernant la résonance paramagnétique électronique (RPE) des défauts placés en substitution dans des oxydes doubles ABO_3 de structure perovskite. Les sites du réseau et les valences des ions substituants sont considérés dans le paragraphe 2. L'existence des paires métal de transition-vacance d'oxygène, $Me-V_O$, et leurs structures atomiques sont analysées dans les paragraphes 3 et 4. La détermination de la position locale de Fe^{3+} au site B dans les cristaux présentant des transitions de phase ferroélectriques est présentée dans le paragraphe 5 tandis que les valeurs anormalement basses du paramètre cubique RPE de Fe^{3+} sont discutées dans le paragraphe 6.

Abstract. — A review is given of electron paramagnetic resonance (EPR) research of substitutional defects in ABO_3 double oxides crystallizing in the perovskite structure. In section 2, the valency and lattice sites are considered. In section 3, the existence of transition metal-oxygen vacancy pairs, $Me-V_O$, is reviewed, and in 4, their atomic structure is analysed. In section 5, the determination of the local position of Fe^{3+} at B sites in crystals undergoing ferroelectric phase transitions is presented, and its anomalously low cubic splitting EPR parameter discussed in 6.

1. **Introduction.** — Electron paramagnetic resonance of transition metal ions in ABO_3 compounds has been used over the past 25 years to study a variety of subjects. These studies provided a deeper insight into the resonance phenomenon itself, as was the case for Fe^{3+} in a cubic crystal field [1], or into the Jahn-Teller effect [2], and they permitted an investigation of structural [3] and ferroelectric phase transitions [4]. This paper is an attempt to summarize the present knowledge of certain defects, in particular the conditions of their occurrence, and their structure.

2. **Valency and lattice sites.** — Double oxides ABO_3 with perovskite structure are nearly all cubic if heated to sufficiently high temperatures; the cubic lattice constants are observed to be around 4 Å. The A ion, with a radius of 1-1.4 Å, is dodecahedrally coordinated by oxygens, and the B ion sits in an oxygen octahedron. Its radius is about half that of the A ion in order to yield a Goldschmidt tolerance factor of $t = \overline{AO}/\sqrt{2}.\overline{BO}$ near unity [5]. Due to these sizes, the transition metal impurities substitute on the B site, and the rare-earth ions on the A sites. Early examples of such EPR studies are Fe^{3+} on the B site and Gd^{3+} on the A site in $SrTiO_3$ [1, 6] and $BaTiO_3$ [4, 6]. However, in $KTaO_3$

single crystals grown from $K_2CO_3-Ta_2O_5$ solutions, Fe^{3+} and Ni^{3+} ions on K^+ sites have been observed [7] apart from normal Ta site occupation. Gd^{3+} on Ti sites has been reported for ceramic $BaTiO_3$ synthetized with enriched Ba *versus* Ti ratios as well as for reduced and quenched $BaTiO_3$ single crystals [8]. Ti^{3+} off-centre on Sr^{2+} sites has been observed in $SrTiO_3$ after neutron irradiation and in one case after reduction [9].

Whereas the rare-earth ions exhibit their known valencies whether they substitute for an A or B site, i.e., Pr^{3+} [10], Gd^{3+} Eu^{2+}, etc. [6], this is not at all the case for the 3d transition metal ions on octahedral B sites. Table I compares the valencies observed in $SrTiO_3$ with those in MgO and CaO. In all three compounds, the stability of the transition ions extends over four valencies. Towards the right, the limit of stability is given by electron loss, towards the left, by hole loss energy.

$$Me^{+n} \rightarrow Me^{n+1} + e$$

$$Me^{+n} \rightarrow Me^{n-1} + h .$$

These boundaries are functions of the electronic deformation and polarization energy E_n, the electron affinity of the bulk crystal χ, the impurity Jahn-Teller energy E_{JT} and crystal-field energies C_N. For MgO and CaO crystals, Stoneham and Sangster [11] accounted for the observed valency span with large-scale computing of E_n, and assuming $\chi = -1$ eV.

Table I. — *References for* : $SrTiO_3$: V^{4+} [12]; Cr^{3+} [13]; Cr^{5+} [14]; Mn^{2+} [15]; Mn^{4+} [16]; Fe^{2+} *by Möss-bauer* [17]; Fe^{3+} [1]; Fe^{4+} *by opt. abs.* [18]; Fe^{5+} [19]; Co^{3+} *by Mössbauer* [17] *and inexistence of* EPR [20]; Ni^{2+} [21]; Ni^{3+} [2], [21]; Ni^{4+} [22]; MgO/CaO [11].

$SrTiO_3$

		V^{4+}		
	Cr^{3+}			Cr^{5+}
Mn^{2+}		Mn^{4+}		
$[Fe^{2+}]$	Fe^{3+}	$(Fe)^{4+}$		Fe^{5+}
	$[Co^{3+}]$			
Ni^{2+}	Ni^{3+}	$(Ni)^{4+}$		

MgO/CaO

Ti^+			
	V^{2+}	V^{3+}	
Cr^+	Cr^{2+}	Cr^{3+}	
	Mn^{2+}		Mn^{4+}
Fe^+	Fe^{2+}	Fe^{3+}	
Co^+	Co^{2+}		
Ni^+	Ni^{2+}	Ni^{3+}	

For $SrTiO_3$, the valencies are one charge unit higher than in MgO and CaO [11]. As it is known from EPR and optical data that the energies E_{JT} and C_N are nearly equal; this charge difference must result from different E_n and especially χ values.

In the early experiments, the one unit higher valencies in $SrTiO_3$ allowed for the first time the detection by EPR of a tetravalent 3d ion, namely, Mn^{4+} ($S = 3/2$) [15]. Later, the EPR of the isoelectronic Fe^{5+} which chemists had usually assumed to be unstable was found. The existence could be proven by measuring the hyperfine field of the ^{57}Fe isotope to be -201.0 ± 3 kG within 5 kG, the same as observed for the isoelectronic $3d^3$ ions Mn^{4+}, Cr^{3+}, and V^{2+}. Furthermore, it is of interest that the electron-spin g value, $g = 2.013$, *exceeds* that of the free spin despite Fe^{5+} being an electron centre (see Fig. 1). The reason is that the energies E_t for charge transfer of an electron from an oxygen p function onto the Fe^{5+} *become lower*

Fig. 1. — The dependence of the g values of the isoelectronic $3d^3$ and $3d^4$-V_O centres as a function of valency from [19] and after [37].

than Mn^{4+} which in turn are lower than Cr^{3+}. These smaller E_t thus yield a larger positive g shift,

$$\Delta g = g - g_{free} \propto 1/E_t .$$

On the other hand, the intra-ionic electron excitations become higher, giving less negative shifts in $\Delta g \propto -1/E_i$ [19].

EPR of Mn^{2+} in $CaZrO_3$ [23], $BaTiO_3$ and $PbTiO_3$ [24] has been assigned to B sites [15], and an axial Mn^{2+} centre in $SrTiO_3$ [25] to A sites [15, 26] charge compensated locally by an unknown defect. The EPR of 4d transition elements on B sites such as Pt^{3+} in $BaTiO_3$ [27], and Mo^{5+} in $SrTiO_3$ [28] have also been observed, the latter ion exhibiting a dynamic Jahn-Teller effect as Ni^{3+} [2].

3. Me-V_O pairs. — In cubic $SrTiO_3$ doped with Fe, strong axial EPR spectra between $g_z = g_\| \simeq 2$ and $g_\perp \simeq 6$ occurred. Their z axes were along mutual perpendicular [100], [010] and [001] directions and could be accounted for by $|\Delta M| = 1$ transitions between $\pm 1/2$ levels resulting from a large axial D splitting of the $S = 5/2$ state, $D(S_z^2 - (1/3) S(S+1))$ with $D \simeq 1.4$ cm^{-1} [29]. They were ascribed to Fe^{3+} ions next to an oxygen vacancy termed V_O (located along [100], etc.). Therefore the pair-centre notation Fe^{3+}-V_O was introduced. This centre was also found in $KTaO_3$ and $PbTiO_3$ with almost the same D splittings [7, 30], and in $BaTiO_3$ [31]. The Fe^{3+}-V_O centre was important for the analysis of critical phenomena in the structural phase transition of $SrTiO_3$. The latter involves temperature-dependent alternate rotations $\varphi(T)$ of oxygen octahedra around the $\langle 100 \rangle$ axes. The Fe^{3+}-V_O centre rotation $\overline{\varphi}(T)$ is 1.6 times smaller than the intrinsic one, but proportional to the intrinsic $\varphi(T)$ near T_c, and could be determined with high precision [32].

Since then, the same kind of transition metal ion-oxygen vacancy centre has also been observed for other ions and different valencies : Co^{2+}-V_O has been reported by Hannon in $KTaO_3$ [33] and in $SrTiO_3$ by Faughnan [34]. The high spin $3d^7$ ion $Co^{2+}(t_{2g})^4(e_g)^3$ yields the g values $g_\| = 2.061 < g_\perp = 4.933$. The isoelectronic $3d^7$, Fe^{1+}-V_O centre has been reported

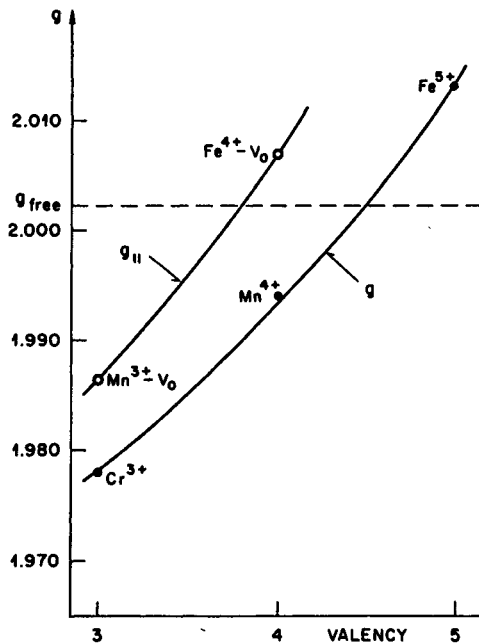by Berney *et al.* [35] most recently in strongly reduced and thermally quenched $SrTiO_3$ after exposing the samples to subband gap light at low temperatures. The measured g values correspond to those observed in the Co^2-V_O centre : $g_\parallel = 1.999 < g_\perp = 4.116$. The other isoelectronic $3d^7$ centre, Ni^{3+}-V_O in $SrTiO_3$ has low spin configuration $(t_{2g})^6 d_{3z^2-r^2}$. The z axis points towards the positively charged vacancy with $g_\parallel = g_z = 2.029 < g_\perp = 2.352$ [36]. Upon illumination with visible light, a new and thermally unstable Ni centre is observed with $g_\parallel = 2.375 > g_\perp = 2.084$. The angle of rotation $\overline{\varphi}(T)$ of the octahedra is the *same* as that of the stable Ni^{3+}-V_O and the Fe^{3+}-V_O centres, and was thus assigned to a Ni^{3+}-V_O centre which has trapped two electrons near the V_O with antiparallel spins (Ni^{3+}-V_O-2 e). The unpaired e_g electron of the Ni^{3+}-V_O-2 e is in a $d_{x^2-y^2}$ orbit, i.e., configuration $(t_{2g})^6 d_{x^2-y^2}$. The average g value is nearly the same as that of the six-fold coordinated Ni^{3+}. The two trapped electrons are thus delocalized from the Ni $d_{3z^2-r^2}$ orbitals — which would otherwise form a $Ni^{1+} (d_{3z^2-r^2})^2 d_{x^2-y^2}$ state — onto the Ti^{4+} ion on the other side of the oxygen vacancy V_O along the z axis. This may also be the case for the Fe^{1+}-V_O centre mentioned above.

Well-oxidized Mn-doped $SrTiO_3$ exhibits only EPR of Mn^{4+} substituting for Ti^{4+}. The reduced crystals, however, indicate cubic Mn^{2+} on Ti^{4+} sites, and two strong axial spectra along general $\langle 100 \rangle$ crystallographic directions [15]. One of them has effective g values of $g_\parallel \simeq 2.00$, $g_\perp^{eff} \simeq 5.9$, and the other $g_\parallel^{eff} \simeq 8$, $g_\perp < 0.4$. The former spectrum is due to the Mn^{2+}-V_O centre with $S = 5/2$, isoelectronic to Fe^{3+}-V_O, and an axial splitting of $D = 0.54$ cm^{-1}. The second centre is quite interesting in its electronic structure. Analysis of this spectrum showed it to be due to a Mn^{3+}-V_O pair. Its orbital wave function is quenched by the strong tetrahedral field into a $B_2(X^2 - Y^2)$ orbital; its spin is $S = 2$, and the large negative D spin splitting $|D| \gg h\nu$ allows EPR observation between the $|2\rangle$, $|-2\rangle$, M_S ground states. The resonance field varies as

$$H_r = [(h\nu)^2 - a^2]/4 g_\parallel \beta \cos\theta,$$

and the hyperfine splitting as $A/4 g_\parallel \beta \cos\theta$. Here θ is the angle between a $\langle 100 \rangle$ direction and the external magnetic field, $g_\parallel^{eff} = 4 g_\parallel$, a is the cubic crystalline splitting, and A the hyperfine interaction constant.

The iron pair-centre, Fe^{4+}-V_O, isoelectronic to the Mn^{3+}-V_O, with high spin $S = 2$, was observed shortly after the latter [37]. Its net charge is $+ 2 e$ and it can be observed in $SrTiO_3$ charge compensated with Mg^{2+}, and Al^{3+} at Ti^{4+} sites. The existence of the Fe^{4+}-V_O had been postulated by Morin and Oliver [38].

In figure 2, the angular dependence of EPR lines due to the Fe^{3+}-V_O and Fe^{4+}-V_O centres is shown for 77 K, i.e. below the 105 K structural phase transition of $SrTiO_3$. The rotation angles $\overline{\varphi}(T)$ of the two centres

are the same. Note that for Fe^{4+}-V_O pairs, an angle-independent line, i.e. the « perpendicular spectrum » is not observed. According to figure 1, the $g_\parallel$ values of the Mn^{3+}-V_O and Fe^{4+}-V_O centres exhibit the same upward trend with increasing valency as is observed in the Cr^{3+}, Mn^{4+}, Fe^{5+} sequence. The reasons are the same as mentioned at the end of section 2, namely, a decrease of the transfer energies with increasing valency. These charge-transfer energies have been determined by the EPR conversion-rate technique. These investigations have been reviewed elsewhere [39].
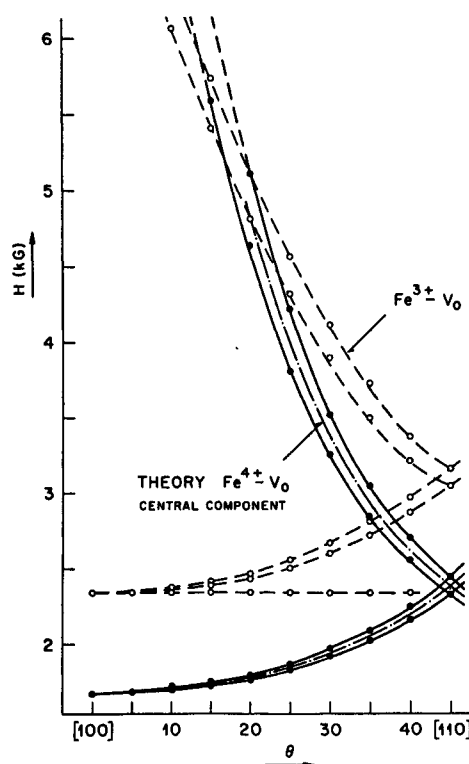
Fig. 2. — Angular dependence of the ESR of Fe^{4+}-V_O and Fe^{3+}-V_O for H in a [100] plane at $\sim$ 19.5 GHz and 4.2 K from [37].

In $SrTiO_3$ reduced at high temperatures and then quenched, another axial centre with even spin S has been seen [35]. Assuming $S = 2$, an axial splitting parameter $D = 9.58$ cm^{-1} was deduced. As the rotation angle $\overline{\varphi} = 1.0°$ at 77 K, it has been assigned to a Fe^{2+}-V_O pair, which upon low-temperature illumination yields the Fe^{1+}-V_O centre. Another Fe^{3+} spectrum of orthorhombic symmetry was also observed [35].

More recently, the neutral Ti^{3+}-V_O centre has been reported in Ti-doped $KTaO_3$ [40] with : $g_\parallel = 1.997 > g_\perp = 1.904$. A centre with $g_\parallel = 1.932 > g_\perp = 1.914$ in flux-grown $BaTiO_3$ [41] doped with La was reassigned to a La^{3+}-V_O-Ti^{3+}

complex [36] and in K^+-doped $BaTiO_3$ [41] to a Ba^{2+}-V_O-Ti^{3+} [36] array. Electron spin resonance results due to holes trapped at oxygen ions and other defects have been reported, but are not related to Me-V_O pairs.

4. Structure of the Fe^{3+}-V_O and Mn^{2+}-V_O pairs. —

The Fe^{3+} and Mn^{2+} ions have a half-filled 3d shell, i.e., their configuration is $3d^5$, and thus the orbital angular momentum L is zero and their electronic spin $S = 5 \times 1/2 = 5/2$. For these ions, the spin-Hamiltonian parameter D in the axial field of the V_O is quite large, namely of the order of a wave number as reviewed in section 3. For reasons beyond the scope of this paper, D is determined by more than 70 % by the next-neighbour ligand positions. Thus, a missing ligand obviously has a drastic effect. If this is the case (which may not apply to less covalently bound ions, i.e., rare-earth ions such as Gd^{3+}), the Newman model involving a superposition of *individual nearest-neighbour* oxygen *contributions* yields the parameters b_2^m with good accuracy [42]. Referring the position of the ligand centres to that of Fe^{3+} by means of polar coordinates R_i, θ_i, φ_i one obtains

$$b_2^m = \overline{b}_2(R_0) \sum_{i=1}^{N} \left(\frac{R_0}{R_i}\right)^{t_2} K_2^m(\theta_i, \varphi_i) \qquad (1)$$

with

$$K_2^0(\theta) = 1/2(3 \cos^2 \theta - 1)$$

$$K_2^2(\theta, \varphi) = 3/2 \sin^2 \theta \cos 2\varphi .$$

In equation (1), R_0 is a reference distance for the intrinsic parameter $\overline{b}_2(R_0)$. For Fe^{3+},

$$\overline{b}_2 (2.101 \text{ Å}) = -0.412(25) \text{ cm}^{-1} ,$$

and the intrinsic exponent $t_2 = 8 \pm 1$ of the model was determined for oxygen ligands using uniaxial-strain EPR data of Fe^{3+} in MgO, and similar data for Mn^{2+} [26].

Recently, Siegel and Müller [26] gained information on the Fe^{3+}-V_O and Mn^{2+}-V_O pair-centre structure using the above model. To compare the different compounds, the quantity $b_2^0/\overline{b}_2(d)$ was used. Here, $b_2^0 \equiv D$ is the measured spin-Hamiltonian parameter, and $\overline{b}_2(d)$ the intrinsic parameter for Fe^{3+} and Mn^{2+}, respectively, and the oxygen ligands at undistorted distance d. It was found that for Fe^{3+}-V_O pair-centres in $SrTiO_3$ [32], $KTaO_3$, and $PbTiO_3$ [30] as well as Mn^{2+}-V_O in $SrTiO_3$ [15], the ratio $b_2^0/\overline{b}_2(d)$ was -2 near $d = 2$ Å. These values were explained with the following model as shown in figure 3 : i) The Fe^{3+} or Mn^{2+} ion can move a distance $\Delta \cdot d$ along the direction of the C_{4v} symmetry axis of the pair-centre; ii) a contraction $(1 - c)\, d$ of the four planar oxygens perpendicular to the Me-V_O axis can occur. It is seen that a broad minimum of -1.4 for $b_2^0/\overline{b}_2(d)$ results
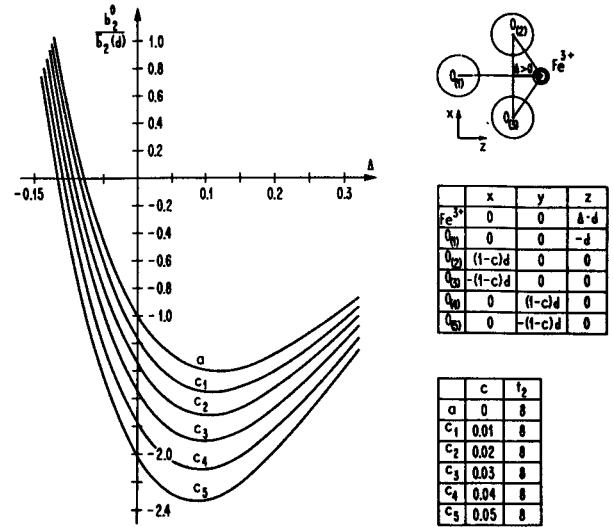

Fig. 3. — Local environment, coordination of the ions, and the prediction of $b_2^0/\overline{b}_2(d)$ for an Me-V_O centre with different contractions of the four planar oxygen ions from [26].

for $c = 0$. When the cation moves towards the vacancy, i.e., $\Delta > 0$, more negative values near -2 are obtained for $c \neq 0$. With a 4 % contraction ($c = 0.04$), a minimum of -2.1 at $\Delta_{min} = 0.09$ is reached. Here, $\Delta = 0.09$ means a displacement of 0.18 Å towards the vacancy for $d = 0.5\, a = 2$ Å. For this curve, the values are -2 to -2.1 in the range from $\Delta = 0.4(0.08$ Å) to $\Delta = 0.15(0.3$ Å). It is therefore understandable that in compounds where the Fe^{3+} and Mn^{2+} movements differ, approximately the same values of $b_2^0/\overline{b}_2(d)$ are reached. The 4 % contraction agrees well with the reduction of the ionic radius of the Fe^{3+} ion by changing the coordination number from 6 to 5 as listed by Megaw [5]. When the Fe ions move towards the oxygen vacancy [26], there is a reduction in the rotation angle $\overline{\varphi}$ of the Fe^{3+}-V_O centre as compared to the intrinsic angle φ, below T_c. As identical rotation angles have been reported [35, 37] for the Fe^{4+}-V_O, Fe^{3+}-V_O and Fe^{2+}-V_O pair-centres, the geometry must be the same. This shows that Coulomb interaction does not play an important role for the centres, as in one case the iron is nominally tetravalent and in the others trivalent and divalent. It follows that the core repulsion is dominant, forcing the metal ion towards the vacancy V_O.

5. Local position of Fe^{3+} in ferroelectric perovskites.

— The most thoroughly investigated ferroelectric crystal in this category is $BaTiO_3$. The ferroelectric phase transition results from the Ti sublattice and the highly polarizable oxygens moving towards each other. The first complete study of Fe^{3+} in the tetragonal phase was carried out by Hornig, Rempel and Weaver [4]. The Fe^{3+} substitutes for the Ti^{4+} on the octahedral

Table II. — EPR *parameters of* Fe^{3+} *in four phases of* $BaTiO_3$.

Crystal structure	Temperature	Refs.	$\underline{a}$ (cm^{-1})	b_2^0 (cm^{-1})	z axis direction	Refs.	Centred Fe^{3+} computed b_2^0 (cm^{-1})
Cubic	160 °C	[4]	+ 0.0102	0	—		
Tetragonal	27 °C	[4]	+ 0.0091	+ 0.0929	$\langle 100 \rangle$ ‖ P	[47]	+ 0.105 ± 0.025
Orthorhombic	− 60 °C	[43]	+ 0.0094	− 0.064	$\langle 001 \rangle$ ⊥ P	[47]	− 0.057 ± 0.014
Rhombohedral	− 196 °C	[44]	+ 0.0115	− 0.0023	$\langle 111 \rangle$ ‖ P	[47]	− 0.0086 ± 0.0022

site, and exhibits a cubic spectrum. Below the cubic (Pm3m) to tetragonal (P4mm) ferroelectric transition at about 120 °C, an axial term, with splitting constant D, along the { 001 } tetragonal domain axes, had to be added to account for the data. Rimai and De Mars [6] related D to the polarization P and obtained $D = 1.6 P^2$ if P is measured in μC/cm^2 and D in units of 10^{-4} cm^{-1}. These authors also doped the crystals with Gd^{3+} ($S = 7/2$) replacing a Ba^{2+} ion. The Gd^{3+} D parameter also varies proportionally to $P^2(T)$ [6].

Subsequent studies by Sakudo [43] and Sakudo and Unoki [44] extended the investigations to the orthorhombic Amm2 and rhombohedral R3m phases of $BaTiO_3$. These results are summarized in the fifth column of table II, which presents a number of remarkable facts : i) The cubic-splitting constant $a \simeq 0.01$ cm^{-1} does not vary more than 10 % across the phase changes. This indicates that the Fe^{3+} sees the same oxygen octahedral environment. ii) Of great importance, the axial $D \equiv b_2^0$ parameter changes sign on going from the tetrahedral to the orthorhombic phases and no orthorhombic term

$$E(S_x^2 - S_y^2) = \tfrac{1}{3} b_2^2 O_2^2$$

appears. The z axis of the O_2^0 term is parallel [100] and lies perpendicular to the polarization axis [011]. iii) The axial D term in the rhombohedral phase is parallel to the polarization ($P \parallel [111]$) but it is one to two orders of magnitude smaller than in the tetragonal and orthorhombic phases, although the polarization is of the same order in all polar phases [45]. Later, Takeda reported on his Gd^{3+} studies in the lower two phases of $BaTiO_3$ [46]. In contrast to the Fe^{3+} results, he found axial $|b_2^0|$ terms directed along $\langle 100 \rangle$ and $\langle 111 \rangle$ axes of almost the same magnitude, 267 and 340 × 10^{-4} cm^{-1}, respectively, as compared to 294 × 10^{-4} cm^{-1} in the tetragonal phase. These splittings are thus perfectly normal in their magnitude as compared to the polarizations observed in the three phases, and their axes are parallel

to the polarization vectors. Takeda computed the field gradients for Gd^{3+} resulting from the neighbour oxygen positions including their polarization, the same as Sakudo [43] for Fe^{3+}, the contributions from the Ti^{4+} being small. Takeda obtained reasonable agreement in assuming oxygen polarizations parallel to $\langle 110 \rangle$ and $\langle 111 \rangle$, whereas Sakudo had to assume oxygen polarizations parallel to $\langle 100 \rangle$ directions in the low symmetry phases. Due to this discrepancy, Siegel and Müller [47] most recently used the Newman superposition model for Fe^{3+} in $BaTiO_3$ to account for the experimental Fe^{3+} b_2^m data of table II, i.e., they neglected the direct influence of the polarization of the oxygens, and took only their position into account, and of greatest importance, they relaxed the assumption of earlier researchers, that the Fe^{3+} has the same lattice coordinates as the Ti^{4+}. In one of their models, they allowed the Fe^{3+} to move freely along the polarization axes by an amount $\Delta \cdot d$. Their investigation gave conclusive evidence that the Fe^{3+} participates by less than an order of magnitude in the collective off-centre Ti^{4+} motion, i.e., it remains at the approximate centre of the octahedron. In the last column of table II, computed values of b_2^0 are listed using equation (1) *without adjustable parameters*. They were obtained with the intrinsic constants $\bar{b}_2(R_0)$ and t_2 given in section 4 and assuming a centred Fe^{3+} in the octahedron using the intrinsic positions of the oxygens as determined from refined X-ray scattering analysis. Note, that with this analysis, a near-axial term with $z \perp P$ in the orthorhombic phase, i.e., $b_2^2 \ll b_2^0$ was obtained. In the rhombohedral $BaTiO_3$ phase, the oxygens are located on an almost undistorted octahedron. As the Fe^{3+} is very near its centre, the axial b_2^0 term almost vanishes. The success of this analysis implies that the polarization fields can be neglected as compared to the effect of the nearest-neighbour positions. It justifies an assumption of Wemple [48] in deriving the $D = 1.4 P^2$ formula from polarization-induced strain only, neglect-

Table III. — EPR *parameters of* Fe^{3+} *in* $PbTiO_3$ *and* $KNbO_3$.

Crystal	Structure	Temperature	Refs.	b_2^0 (cm^{-1})	z axis direction	Refs.	Centred Fe^{3+} computed b_2^0
$PbTiO_3$	tetragonal	300 K	[49]	+ 0.53 ± 0.02	$\langle 100 \rangle$ ‖ P	[47]	+ 0.58 ± 0.14
$KNbO_3$	orthorhombic	300 K	[50]	| 0.18 ± 0.001 |	$\langle 001 \rangle$ ⊥ P	[47]	− 0.15 ± 0.04
				| b_2^2/D | = 0.17		[47]	| b_2^2/D | = 0.12 ± 0.1

ing the direct polarization effect on the centred Fe^{3+} ion.

Analog results to $BaTiO_3$ were also obtained for Fe^{3+} in $PbTiO_3$ and $KNbO_3$ [47]. Table III compiles the known experimental Fe^{3+} EPR parameters of $PbTiO_3$ in the tetragonal [49] and $KNbO_3$ in the orthorhombic phases [50], and compares them to the computed values assuming the Fe^{3+} to be at the centre of the oxygen octahedron. The agreement is again very satisfactory.

The reduced Fe^{3+} participation in the collective Ti^{4+} motion implies that on doping, the transition temperature T_c of $BaTiO_3$ must be strongly reduced. This property was indeed found : 1 % doping reduced T_c by 15 K [51] ; the effect of creating V_O's, which also reduce T_c, has been subtracted [52].

The Fe^{3+} contains five 3d electrons ($3d^5$) in anti- or non-bonding orbitals. They impede bonding of the oxygen p electrons with the empty 3d orbitals, possible in Ti^{4+} ($3d^0$) or $Nb^{4+}(4d^0)$. This points to the very origin of displacive ferroelectricity which is mainly found in oxides containing ions with empty d orbitals. The size and charge of an ion are also important. Zr^{4+} has an empty $4d^0$ orbital like Nb^{5+} but upon doping into $BaTiO_3$ suppresses T_c because its size 0.72 Å is 0.12 Å larger than that of Ti^{4+}. However, it depresses T_c less than Sn^{4+} [45] with a radius of only 0.69 Å but a full $4d^{10}$ shell [5]. This shows that for Zr^{4+}, the empty 4d shell, which is favourable to ferroelectricity, counteracts the suppressive effect of the large size. We can interpret recent doping experiments of $BaTiO_3$ by Hagemann and Ihrig [52] in the same manner : Zn^{2+} doping depresses T_c by 15 K/ mol. %, whereas Ni^{2+} doping lowers T_c by 30 K/ mol. %. The radius of the former ion is larger, being 0.75 Å, the latter only 0.69 Å, thus, Ni^{2+} should depress T_c less if it depended only on the effect of size and creation of V_O's. In our opinion, the enhanced depression observed with Ni^{2+} results from its almost full 3d shell with configuration $3d^8$. The Ga^{3+} and Fe^{3+} doping experiments of reference [52] can be discussed in a similar manner.

6. The EPR parameter a in $BaTiO_3$ and $KNbO_3$.

— The a parameters shown in table II are about a factor 2.5 smaller than those measured in normal cubic oxides with the same cation-anion distance. This fact and its possible implication remained unnoticed
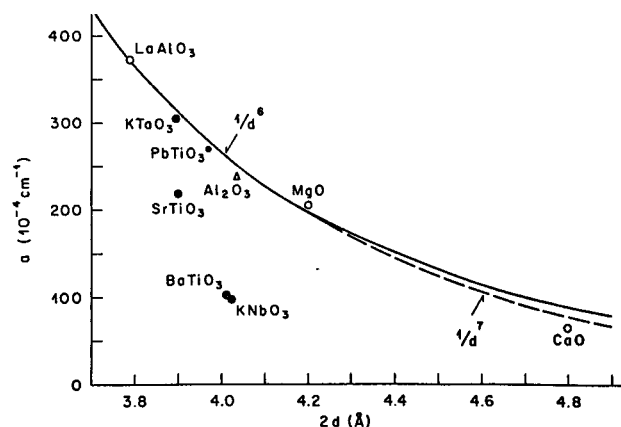

Fig. 4. — EPR cubic splitting parameter a of Fe^{3+} at octahedral sites in oxides as a function of average double cation-anion lattice distance 2 d. The symbols O, ● refer to cubic oxide sites without and with ferroelectric soft modes, respectively ; △ to trigonally distorted octahedral sites in an oxide without a soft mode (from [53]).

for several years. In $BaTiO_3$, the soft ferroelectric mode is overdamped and anisotropic in the cubic phase as in $KNbO_3$, which shows the same set of three phase transitions. Thus, the EPR of Fe^{3+} in $KNbO_3$ was investigated experimentally by Siegel et al. [50]. The only phase where results are available so far, is at room temperature, i.e., in the orthorhombic phase. It turned out that a is essentially the same as in $BaTiO_3$. In figure 4 measured a parameters in near-cubic oxides are compared and shown to vary systematically as a function of the intrinsic lattice constant d [53]. They follow a $a = a_0/d^7$ law, irrespective of the nominal charge of the ion which the Fe^{3+} replaces. The anomalously low value of a in $BaTiO_3$ and $KNbO_3$ is striking and could be a microscopic test quantity for ABO_3 ferroelectrics with Slater-type B-ion motion. The above statement is further supported by recent EPR measurements by Rytz et al. in mixed crystals, $KTa_{1-x}Nb_xO_3$ [54] for $0 \leqslant x < 0.15$. Although the lattice constant d remains essentially the same, the EPR parameter a decreases linearly with x from the pure $KTaO_3$ value of $0.030\ 5\ cm^{-1}$ and extrapolates to $0.010\ cm^{-1}$ for pure $KNbO_3$. It is interesting to note that the ferroelectric transition temperature increases linearly with x [55].

References

[1] MUELLER, K. A., Helv. Phys. Acta 31 (1958) 173.

[2] SLONCZEWSKI, J. C., MUELLER, K. A. and BERLINGER, W., Phys. Rev. B 1 (1970) 3545.

[3] MUELLER, K. A., von WALDKIRCH, Th., in Local Properties at Phase Transitions, Proceedings of Enrico Fermi Int. School of Physics (North Holland, Amsterdam) 1976, p. 187.

[4] HORNIG, A. W., REMPEL, R. C. and WEAVER, H. E., J. Phys. Chem. Solids 10 (1959) 1.

[5] MEGAW, H. D., Crystal structures : A working approach (W. B. Saunders, London, England) 1973.

[6] RIMAI, L. and DE MARS, G. A., Phys. Rev. 127 (1962) 702 ; and in Proceedings of the 1st. International Conference on Paramagnetic Resonance, W. Low Ed. (Academic Press, N. Y.) 1963, p. 51.

[7] HANNON, D. M., Phys. Rev. 164 (1967) 366.

[8] TAKEDA, T. and WATANABE, A., J. Phys. Soc. Japan 19 (1964) 1742 and ibid. 21 (1966) 1132.

[9] Schirmer, O. F. and Mueller, K. A., Phys. Rev. B 7 (1973) 2986;
Van Engelen, P. P. J. and Henning, J. C. M., Phys. Lett. 25A (1967) 733.

[10] Graenicher, H., Huebner, K. and Mueller, K. A., Helv. Phys. Acta 30 (1957) 480.

[11] Stoneham, A. M. and Sangster, M. J., preprint (1980).

[12] Kool, T. W. and Glasbeek, M., Solid State Commun. 32 (1978) 1099.

[13] Mueller, K. A., Arch. Sci. Genève 11 (1958) 150.

[14] Mueller, K. A., Magnetic Resonance and Related Phenomena, Proceedings 16th Congress Ampère, 1971, I. Ursu Ed., (Rumanian Acad. Sci.) p. 173.

[15] Serway, R. A., Berlinger, W., Mueller, K. A. and Collins, R. W., Phys. Rev. B 16 (1977) 4761.

[16] Mueller, K. A., Phys. Rev. Lett. 2 (1959) 341.

[17] Bhide, V. G. and Bhasin, H. C., Phys. Rev. 172 (1968) 290 and references therein.

[18] Faughnan, B. W., Phys. Rev. B 4 (1971) 3623, Blazey, K. W., Phys. Status Solidi 38 (1976) K 97.

[19] Mueller, K. A., von Waldkirch, Th., Berlinger, W. and Faughnan, B. W., Solid State Commun. 9 (1971) 1097.

[20] Mueller, K. A. and Berlinger, W., unpublished.

[21] Rubins, R. S. and Low, W., Proceedings of the 1st. International Conference on Paramagnetic Resonance, W. Low Ed. (Academic Press, N. Y.) 1963, p. 59.

[22] Koidl, P., Blazey, K. W., Berlinger, W. and Mueller, K. A., Phys. Rev. B 14 (1976) 2703.

[23] Henderson, B., Proc. Phys. Soc. London 92 (1967) 1064.

[24] Ikushima, H. and Hayakawa, S., J. Phys. Soc. Japan 27 (1969) 414 and references therein.

[25] Hannon, D. M., Phys. Rev. B 3 (1971) 2153.

[26] Siegel, E. and Mueller, K. A., Phys. Rev. B 19 (1979) 109.

[27] Sroubek, Z., Zdansky, K. and Simanek, E., Phys. Status Solidi 3 (1963) K1.

[28] Faughnan, B. W., Phys. Rev. B 5 (1972) 4925.

[29] Kirkpatrick, E. S., Mueller, K. A. and Rubins, R. S., Phys. Rev. 135 (1964) A86

[30] Wessel, G. and Goldick, H., J. Appl. Phys. 39 (1968) 4855; Lewis, O. and Wessel, G., Phys. Rev. B 13 (1976) 2742.

[31] Gainon, D. J. A., J. Appl. Phys. 36 (1965) 2325.

[32] Von Waldkirch, Th., Mueller, K. A. and Berlinger, W., Phys. Rev. B 5 (1972) 4324.

[33] Hannon, D. M., Phys. Status Solidi (b) 43 (1971) K21.

[34] Faughnan, B. W., RCA Internal Reports (1969), unpublished.

[35] Berney, R. L., Cowan, D. L. and Morin, F., Solid State Commun. 26 (1978) 579. The interpretation of the g values for the $Fe^{1+}-V_O$ centre can be carried out as done for $Co^{2+}-V_O$ in references [33] and [34]. A detailed account including photochromic studies appeared most recently : Berney, R. L. and Cowan, D. L., Phys. Rev. B 23 (1981) 37.

[36] Mueller, K. A., Berlinger, W. and Rubins, R. S., Phys. Rev. 186 (1969) 361.

[37] Schirmer, O. F., Berlinger, W. and Mueller, K. A., Solid State Commun. 16 (1975) 1289.

[38] Morin, F. J. and Oliver, J. R., Phys. Rev. B 8 (1973) 5847.

[39] Mueller, K. A., Proceedings IV Ampère International Summer School on Magnetic Resonance in Condensed Matter-Recent Developments, Pula, Yugoslavia (1977), Eds. R. Blinc and G. Lahajnar (Univ. of Ljubliana, Yugoslavia) p. 663.

[40] Geifman, I. N., Phys. Status Solidi (b) 85 (1978) K5.

[41] Takeda, T. and Watanabe, A., Japan. J. Appl. Phys. 7 (1968) 232 and references therein.

[42] Newman, D. J. and Urban, W., Adv. Phys. 24 (1975) 793; Newman, D. J. and Siegel, E., J. Phys. C : Solid State 9 (1976) 4285.

[43] Sakudo, T., J. Phys. Soc. Japan 18 (1963) 1626.

[44] Sakudo, T. and Unoki, H., J. Phys. Soc. Japan 19 (1964) 2109.

[45] Jona, F. and Shirane, G., Ferroelectric Crystals (Pergamon, London) 1962, p. 249.

[46] Takeda, T., J. Phys. Soc. Japan 24 (1968) 533.

[47] Siegel, E. and Mueller, K. A., Phys. Rev. B 20 (1979) 3587.

[48] Wemple, S. H., MIT Technical Report 425 (1962) 53.

[49] Pontin, R. G., Slade, E. F. and Ingram, D. J. E., J. Phys. C 2 (1969) 1146.

[50] Siegel, E., Urban, W., Mueller, K. A. and Wiesendanger, E., Phys. Lett. 53A (1975) 415.

[51] Ihrig, H., J. Phys. C 11 (1978) 819.

[52] Hagemann, H. J. and Ihrig, H., Phys. Rev. B 20 (1979) 3871.

[53] Mueller, K. A., Phys. Rev. B 13 (1976) 3209.

[54] Rytz, D., Boatner, C. A., Chatelain, A., Hoechli, U. T. and Mueller, K. A., Helv. Phys. Acta 51 (1978) 430.

[55] Triebwasser, S., Phys. Rev. 114 (1959) 63.